Mechanochemical synthesis of inverse vulcanized polymers

Peiyao Yan[‡*1], Wei Zhao[‡1, 2], Fiona McBride[3], Diana Cai[1], Joseph Dale[1], Tom Hasell[*1]

[1]Department of Chemistry, University of Liverpool, Crown Street, Liverpool L69 7ZD (UK); [2]Leverhulme Research Centre for Functional Materials Design, Materials Innovation Factory and Department of Chemistry, University of Liverpool, Liverpool (UK); [3] Surface Science Research Centre, University of Liverpool, Liverpool L69 3BX (UK).

Abstract:

Inverse vulcanization, a sustainable platform, can transform an industrial by-product, sulfur, into polymers with broad green applications such as heavy metal capture and recyclable materials. However, the process usually requires high temperatures (≥159 °C), and the crosslinkers needed to stabilise the sulfur are therefore limited to high-boiling-point monomers only. Here, we report an alternative route for inverse vulcanization — mechanochemical synthesis (MS), with advantages of mild conditions (room temperature), short reaction time (3 h), high atom economy, less H_2S, and broader monomer range. Successful generation of polymers using crosslinkers ranging from aromatic, aliphatic to volatile, including renewable monomers, demonstrates this method is powerful and versatile. Compared with thermal synthesis, the MS products show enhanced mercury capture. The resulting polymers show thermal and light induced recycling. The speed, ease, versatility, safety, and green nature of this process offers a more sustainable future for inverse vulcanisation, and enables further unexpected discoveries.

Introduction:

Elemental sulfur, as a by-product during the hydrodesulfurization process of crude oil, is extensively produced but has incomplete usage despite its main application in the production of sulfuric acid.[1, 2] Hence, there is an urgent need to explore an efficient way to transform this waste into useful materials. Recently, 'inverse vulcanization' coined by Pyun and co-workers has given a feasible solution to this issue as more than 50 wt.% sulfur can be used when a sulfur-containing polymer is formed using this process.[3] The polymers generated by this polymerization route are a new category of material based on a sulfur-sulfur back-bone rather than carbon-carbon back-bone. Consequently, they show many unique properties thanks to their special polymer structures, such as having the highest refractive index among organic materials,[4, 5, 6, 7] showing good recycling ability despite having crosslinked structures,[8, 9, 10, 11] possessing excellent heavy metal sensitivity arising from the sulfur content,[12, 13, 14, 15] and showing antibacterial activity thanks to sulfur hybridization[16, 17, 18]. Starting from the waste material and turning towards functional applications, inverse vulcanization acts as a sustainable platform of science and technology gives the plastics more sustainable future. Since the first research publication was reported, there has been much related research upon both the underlying chemistry and theoretical, and the potentially applicable directions and applications.[19, 20, 21] Majority of renewable resources have been used for production of useful sulfur polymers to be applied in the green areas.

Normally, inverse vulcanized polymers are produced through bulk polymerization at high temperature (≥159 °C), because of the requirements for the cleavage of S-S bonds to enable ring opening and subsequent polymerisation of the eight-membered ring (S_8) by heating. However, there are many accompanying problems in this polymerization process including but not limited to: inhomogeneous polymers obtained caused by less miscible monomers or different reactivity of monomers at high temperature, uncontrollable auto-acceleration[22], side reactions accompanied by hydrogen abstraction and H_2S generation[23], and the limitation of co-

monomer choice by boiling point. That is unsafe and hazardous in the operation. In order to apply this new material industrially, alternative easier and safer synthesis methods should be explored. Some attempts have been made regarding to this issue, for example, catalytic synthesis lowered the reaction temperature and unlocked some new monomers, but more than 100 °C is still needed;[24, 25] also, a vapor-phase deposition method which offers an opportunity for more homogeneous reaction and expanded crosslinker range, but it still requires high temperature and harsh conditions.[5]

Here, we have demonstrated that the mechanochemical synthesis (MS), a green method, can be used into the production of inverse vulcanized polymers by using ball milling. Mechanochemistry has a long history from the primaeval mortar and pestle used since the stone age onward.[26, 27, 28, 29] Laboratory shaker mills were introduced into chemistry research since the last century and have enabled substantial progress. Up to date, mechanochemistry using ball milling has been extensively exploited in organic synthesis,[30, 31] inorganic synthesis[32, 33] and materials synthesis.[34, 35] This technique is sourced from mechanical energy and is an environmentally-friendly method which shows advantageous properties including shorter reaction time, homogeneous reaction, high atom economy and so on. It is investigated here for the first time for the synthesis of inverse vulcanised polymers by the MS method. No requirement for heating, fast reaction, solvent-free, reduced hydrogen abstraction, no auto-acceleration, broader monomer options, and more homogeneous reaction regardless of miscibility of sulfur with monomers can all be observed in this polymerization method. According to the obtained results, in addition to the process advantages the method possesses, the polymer materials obtained by the MS method show many unexpected and interesting properties compared with the normal thermally synthesized products, which are discussed in detail below. A notable and surprising finding was that the fallen iron filings from the steel

milling balls are able to chemically react with the polymers to form thermally stable inorganic substances rather than being only physically dispersed in the polymers.

Results and discussions:

We synthesized 9 polymers using a ball mill, starting from different crosslinkers ranging from aromatic, aliphatic to volatile monomers including 1,3-diisopropenylbenzene (DIB), dicyclopentadiene (DCPD), divinylbenzene (DVB), 5-ethylidene-2-norbornene (ENB), limonene, myrcene, dially disulfide (DADS), styrene and isoprene (Fig. 1). The synthetic polymers were named as MS(S-monomer) respectively. In addition, 8 polymers derived from the same monomers, omitting isoprene which is unable to be used at high temperature, were synthesized using the conventional thermal synthesis (TS) method to act as control group, and were named as TS(S-monomer) respectively. The experimental procedures of the materials synthesis can be found in the supporting information (SI). MS(S-DIB) and MS(S-Styrene) were used as model reactions to optimize the reaction procedure, as DIB is a well-known monomer, which can chemically stabilize polymeric sulfur, and styrene is a monomer with lower stabilizing efficiency for sulfur because of the lower number of reactive bonds relative to the molecular mass, and linear resulting structure. As differential scanning calorimetry (DSC) curves in Fig. S1 show, the obtained polymer MS(S-DIB) shows a clear glass-rubber transition even after only 1-hour of reaction, and a clear increase of glass transition temperature (T_g) from -11 °C to -1 °C with the reaction time increase from 1 hour to 3 hours, suggesting that DIB can react with sulfur quickly to form sulfur-polymer by ball milling, and further crosslinking reaction occurs during extended reaction time. However, MS(S-Styrene) still has an obvious melt peak of unreacted crystalline sulfur even after 2-hours reaction, and there is only a slight glass-rubber transition apparent. After reacting for 3 hours, there is no unreacted crystalline

sulfur remaining in polymerization system, and the product has a very clear glass-rubber transition. That indicates that styrene needs longer time to fully react with sulfur compared with DIB, and is able to form a sulfur polymer after 3-hours reaction.

Hence, based on the results of optimisation experiments, all other polymers were synthesized for 3 hours in order to fully convert the S_8. To be clear here, all the characterizations of the products were carried out once the polymers were formed without any further treatment unless there is a special illustration. The DSC curves of all the polymers (Fig. S2) show that every polymer has a clear T_g and almost all polymers have no unreacted crystalline sulfur remaining except a slight sulfur melt peak in MS(S-Myrcene) after 3-hours polymerization. It's worth noting that the volatile monomer isoprene (b.p. 34 °C) was proven to successfully react with sulfur to form sulfur polymer by MS method here, which definitely cannot be realised through the conventional thermal synthesis process. Comparing the T_g of MS products with that of TS products (Fig. S3), it is interestingly found that some of the MS products have much lower T_g than the relevant TS products synthesized from the crosslinkers including DIB, DCPD, DVB, ENB and DADS, which would form crosslinked network normally, but other MS products formed from monomers including myrcene, limonene and styrene, show slightly higher T_g than the relevant TS products which are tend to be formed as linear polymer normally. From the powder x-ray diffraction (PXRD) curves of the MS products in Fig. S4, we can see that there is a trace of crystalline sulfur persisting in some of the polymers although it is not apparent from the second heating cycle in DSC curves. The unreacted sulfur can be removed by Soxhlet extraction in acetone as evidenced by the absence of peaks in PXRD patterns (Fig. S5a) of the MS products after Soxhlet extraction, but it needs to be mentioned that further reaction could occur during heating resulting from the dynamic disulfide bonds, since the DSC results (Fig. S5b) which show an increase of T_g of all the polymers after Soxhlet extraction. Hence, all the characterizations of MS polymers were done directly after 3-hours reaction in the ball mill to

investigate their true chemical and physical properties and applications. According to solubility evaluation results in Fig. S6, all the MS polymers were demonstrated to be insoluble in neither tetrahydrofuran (THF), chloroform or acetone, which is notable. As Fig. S7 shows, TS(S-Myrcene), TS(S-Limonene), and TS(S-Styrene), which either exhibit linear or branched rather than fully crosslinked structures, are fully soluble in THF and chloroform and partly soluble in acetone. Other TS polymers, which are more highly crosslinked, are insoluble or only partly soluble in those three solvents. Theoretically, higher crosslinking degree will give higher T_g and higher solvent resistance to the polymer. Here one question arises, why should some of the MS polymers possess lower T_g than the TS polymers, but show higher solvent resistance? Elemental analysis results in Table S2 shows that most of obtained polymers contain high sulfur content but there are changes on the ratios of C:H and C:S after polymerization. The most suspected way which can cause elemental ratio change is the side reaction—H_2S gas generation in thermal synthesis, which can cause C:H ratio and C:S ratio increase as elements S and H are lost. However, the C:H ratio and C:S ratio here both decreased after MS. So, another question comes up—how this happened? Both questions suggest there might be something different from MS method to the normal TS method in mechanism.

In order to investigate these questions and better understand the nature of the chemical reaction in the ball mill, styrene was chosen as model monomer to monitor the reaction as it theoretically has the least reactive activation point. Fourier transform infrared spectroscopy (FT-IR), hydrogen nuclear magnetic resonance spectroscopy (^{1}H NMR), and X-ray photoelectron spectroscopy (XPS) were used to monitor the chemical environment changes as a function of reaction time. From FT-IR curves in Fig. 2A, it is observed that the peak at ~1626 cm^{-1} belonging to the C=C stretch and peaks at ~989 cm^{-1} and ~906 cm^{-1} belonging to C=C bend both disappeared with the increase of the reaction time, which suggests that vinyl groups in styrene were consumed to form polymer. Meanwhile, there is no change of the peaks belonging

to the benzene ring, suggesting that there is no reaction occurring between the benzine group and sulfur, but there is a new peak at ~1701 cm^{-1} appearing after reaction, which is attributed to a C=O group. The same results can be observed from the FT-IR spectra of TS(S-Styrene) (Fig. S8). In addition, DSC curve (Fig. S9) of the control experiment MS(S-Toluene) suggests that there is no reaction between sulfur with saturated hydrocarbon. Due to insoluble property of the MS(S-Styrene), it is difficult to obtain the structure information of the produced polymer using solution NMR, but it is clear that the monomer styrene is fully consumed after 3-hours reaction from the ^{1}H NMR spectra (Figs. S10 and S11) of monomer and products, resulting from the disappearance of the peaks belonging to hydrogen protons of styrene. In addition, energy dispersive spectroscopy (EDS) was used to detect the elements existing in the polymers. It is surprisingly found that there is Fe present in addition to the elements S and C in the polymer from the EDS images of MS(S-DIB) in Fig. 2B. That indicates that there are some iron extracted from steel balls trapped in the polymers, and there is a trace of Cr associated with Fe existing in the polymer, which is normally used in steel production. Moreover, Fig. S12 indicates that Fe was not uniformly dispersed in the polymer. In this case, anchoring of the polymeric products to Fe was considered to be the probable reason for the insolubility and unexplained elemental analysis results of MS products. The presence of the Fe impurities prohibits the use of solid-state NMR. Hence, XPS was used to investigate bonding information of the MS polymers by recording the C 1s, S 2p, Fe 2p and O 1s regions (Fig. 2C). As Fig. S13 shows, clearly there are more S and C chemical environments observed from MS(S-DIB) or MS(S-Styrene) than that of TS(S-DIB) and TS(S-Styrene). Fig. 2F clearly shows the presence of Fe in the polymer MS(S-Styrene), and Figs. 2D and 2E give the detailed connectivity information of polymer MS(S-Styrene). XPS S 2p peak in Fig. 2D is fitted by three components: neutral S (163-165.2 eV) and cationic S^{+} (165.3-166.7 eV) and oxidized SO^{3-} (166.8-168.4 eV)[36]. The S 2p spectrum was curve fitted, indicating the presence of four sulfur chemical

bonding environments; S-S, C-S, S-O and S with Fe at a binding energy (BE) of 163.8 eV, 165.0 eV, 165.4 eV/166.6 eV and 166.9 eV /168.1 eV, respectively[5, 37, 38]. Furthermore, the bonding assignments from the C 1s data, Fig. 2E, show five carbon bonding environments; C-C, C-S, C-O, C=O and metal carbonate at a BE of 284.7 eV, 285.5 eV, 286.4 eV, 287.9 eV, 289.3 eV respectively.[36, 39] That means that sulfur has reacted with the organic co-monomers and chemically connected with carbon to form C-S bonds, and there are bonds of metal sulfonate and metal carbonate formed in the meantime. In contrast, XPS S 2p and C 1s regions (and accompanying survey scan) of TS(S-Styrene) (Fig. S13d) show no Fe present, carbon and sulfur were only observed in only the following bonding environments; S-S (163.9 eV), C-S (165.0 eV in S 2p spectrum and 285.49 eV in C 1s spectrum), and C-C (284.7 eV in C 1s spectrum). Hence, it is further demonstrated that new covalent bonds of C-S were formed in MS polymer, and Fe not only disperses in the polymer physically but chemically connects with the polymer chains. Moreover, XPS spectra of MS(S-DIB) and TS(S-DIB) show similar results with that of MS(S-Styrene) and TS(S-Styrene) (Figs. S13a and S13b). Therefore, all the above proof illustrates that sulfur did react with C=C bonds in the monomers initiated by mechanical energy to successfully form the sulfur polymers, and iron from the steel balls reacted with the polymer to form some inorganic proportion accompanying the polymer formation rather than only being ground iron dispersed among polymer particles, which is surprising and interesting.

Solution inductively coupled plasma optical emission spectrometry (ICP-OES) was used to analyse Fe content of the polymers. As Table S3 shows, there are ranging from 8 wt.% to 20 wt.% Fe in the polymers but there is only 0.77 wt.% Fe in the control sample--ball milled pure elemental sulfur. Furthermore, thermogravimetric analysis (TGA) of MS polymers in N_2 shown in Fig. S14 illustrates that there still are some residue percent from polymers at 1000 °C, but only around 1.4% residue of control sample (ball milled sulfur) was obtained. It is revealed that Fe only reacts with polymer chains during polymer formation but does not react with pure

sulfur. Now, we can understand that why the ratios of C:H and C:S decrease after polymerization in EA results. That is because that percentage of metal cannot be detected using EA technic, but the total percentages of elements were calculated basing on total polymers' mass, which causes decrease of carbon percentage. In addition, unreacted monomers were washed out by acetone before the EA characterization, which further decreases the carbon percentage. Hence, the detected carbon percent is lower than the calculated value so that the ratios of C:H and C:S are lower than the calculated values. That also indicates that there may be no/less H_2S formation during reaction as there is no decrease of sulfur percentage. Theoretically, the organic material all can be burned off in the air. However, the synthesized materials in this case still have Fe oxide remaining after being burned, which can be proved by the EDS images of burned MS(S-DIB) in Fig. S15, there is only elements Fe, Ge or some C which cannot be confirmed since the background is carbon film, but no sulfur remaining. Hence, it is clear that an inorganic fraction formed and iron from the steel balls cause the questions discussed above. Fe reacted with the polymer chain and causes structure change to the polymer resulting in insolubility, where Fe acts as a kind of crosslinker to link the polymer chain into the network. While, the FT-IR curves of some of the polymers in Figs. S16-20 show that partial reaction of C=C of monomer containing 2 or more vinyl groups causes those MS polymers to have lower T_g than the TS polymers. Whereas, some monomers which potentially form highly linear structured polymer, like styrene which has the least C=C so that it has high sulfur rank and high opportunity for Fe to attend the reaction to form high content of inorganic fractions, resulted in the formed polymer having higher T_g than the TS polymer.

In addition, H_2S gas measurements were done to evaluate the hydrogen adsorption in both of MS and TS polymerization. As it is hard to monitor the reaction during the reaction due to the practical limitations of the equipment, the products were used to analyse H_2S generation tests. Polymers TS(S-DIB), TS(S-DCPD), TS(S-DVB) and TS(S-ENB) were chosen as the control

samples to compare with the MS polymers from the same crosslinker respectively, as they all are solid state at room temperature. From Fig. 3A, it can be seen that H_2S is only generated under heating. Slight H_2S concentration can be detected from some of MS products once the temperature reaches 80 °C, but a significant H_2S concentration can be detected when the temperature is 140 °C no matter whether MS polymers or TS polymers. MS products show quicker H_2S generation rate than TS products as they are smaller particles with higher surface area and shorter diffusion pathways. Even through the TS polymers are fully crosslinked polymers, there was significant H_2S generation at high temperature. This suggests that H_2S gas is likely released during the TS process thanks to the high reaction temperature (normally higher than 140 °C). Instead, it can be considered as that there is likely no/less H_2S gas generated during the MS process due to absence of heating. Additionally, the H_2S concentrations released from MS polymers are all higher than that from TS polymers (the data for every polymer can be found in Figs. S24-S31). In theory, less gas generated from the products suggests hydrogen abstraction may have already occurred during the synthesis process as the same monomers and ratio were used in synthesis. Therefore, for the reaction itself, there should be less or no H_2S generated during the MS process, in comparison to the TS process. Moreover, scanning electron microscopy (SEM) images of the MS polymers (Figs. S32-S39) show all the polymers are relatively small size particles. Accordingly, the obtained polymer powders were considered as a sorbent in water remediation. Hence, mercury (Hg) uptake tests were carried out using all the MS polymers with the control samples of solid-state TS polymers and pure sulfur. The experimental procedures of Hg uptake can be found in the SI. As Figs. 3B show, all the MS polymers have higher Hg capture efficiency than the TS polymers as well as pure sulfur. The highest ratio 62% Hg was removed from 138 ppm $HgCl_2$ solution by the polymer MS(S-Myrcene) in 24 hours and the highest capacity of 42.3 mg/g was obtained, which is higher than normally non porous sulfur polymers and even higher than some kinds of

porous polymers reported[22, 40, 41], such as salt templated sulfur polymer which has the capacity of 2.27 mg/g.[40] Additionally, the MS polymer powders can be processed furtherly by hot pressing into polymer thin film, as shown in Fig. 3C, despite their crosslinked structures. As the polymers contain disulfide bonds, the polymer thin film was expected to have potential for healing. It is known that dynamic reaction between the disulfide bonds can be introduced by heat[42] and also ultraviolet (UV) light[43]. Thermally-induced healing properties of inverse vulcanized polymers has been widely investigated[8, 9], but we demonstrate here first time that the inverse vulcanized polymer is able to be self-healed under UV light irradiation. Fig. 3D indicates that two pieces of MS(S-ENB) films were healed together after radiation using 285 nm UV light for 40 minutes. The healed film shows a good elastic property as the video S1 shows, where the film can be stretched and then the deformation can be recovered automatically once the force is released.

Conclusion:

It has been demonstrated that inverse vulcanized polymers can be synthesized using a mechanochemical method. In the conventional thermal synthesis of inverse vulcanised polymers, the choice of potential crosslinkers is constrained to those that are miscible with molten sulfur as well as having sufficiently high boiling points[44]. The mechanochemical route removes these constraints. It was proven that iron from steel balls can react with the sulfur polymer to form inorganic sections anchoring the polymers. The obtained polymers were demonstrated to show many modified properties such as high solvent resistance and high mercury uptake efficiency and capacity. The synthetic materials also show good processing ability which might be used to broaden applications not limited to UV-induced self-healing. Compared with the normal thermal synthesis, mechanochemical synthesis method of inverse

vulcanization is able to give broader monomer choice and promising product range simply starting from the by-product, sulfur, to wider applications.

Corresponding authors:

Tom Hasell: T.Hasell@liverpool.ac.uk

Peiyao Yan: Peiyao.Yan@liverpool.ac.uk

Author contribution:

Materials synthesis and characterizations were performed by P. Y. Yan and W. Zhao; (P. Y. Yan[⊥] and W. Zhao[⊥] contributed equally to this work); F. McBride helped in XPS data analysis; D. Cai helped in mercury capture experiments and results analysis; Joe helped in H_2S gas measurement contact and results analysis, and did TGA technic assistant. T. Hasell directed the project and revised the paper manuscript. Manuscript was prepared by all the authors.

Acknowledgement:

P.Y. Yan and D. Cai thank to the China Scholarship Council (CSC) for awarding them the scholarships. We thank to Keith Arnold for support in EDS images capturing, Steven Moss for ICP-OES analysis, the institute HarwellXPS for support in XPS operation, the institute Anatune for support in H_2S gas measurements. We are grateful to Andrew Cooper generous support of facilities and useful discussions.

References:

1. Ober JA. Materials flow of sulfur. (2002).

2. Griebel JJ, Glass RS, Char K, Pyun J. Polymerizations with elemental sulfur: A novel route to high sulfur content polymers for sustainability, energy and defense. *Progress in Polymer Science* **58**, 90-125 (2016).

3. Chung WJ, *et al.* The use of elemental sulfur as an alternative feedstock for polymeric materials. *Nat Chem* **5**, 518-524 (2013).

4. Kleine TS, *et al.* High refractive index copolymers with improved thermomechanical properties via the inverse vulcanization of sulfur and 1, 3, 5-triisopropenylbenzene. *ACS Macro Letters* **5**, 1152-1156 (2016).

5. Jang W, *et al.* One-step vapor-phase synthesis of transparent high refractive index sulfur-containing polymers. *Sci Adv* **6**, eabb5320 (2020).

6. Kleine TS, *et al.* 100th Anniversary of Macromolecular Science Viewpoint: High Refractive Index Polymers from Elemental Sulfur for Infrared Thermal Imaging and Optics. *ACS Macro Letters* **9**, 245-259 (2020).

7. Kuwabara J, Oi K, Watanabe MM, Fukuda T, Kanbara T. Algae-Inspired, Sulfur-Based Polymer with Infrared Transmission and Elastic Function. *ACS Appl Polym* **2**, 5173-5178 (2020).

8. Griebel JJ, *et al.* Dynamic Covalent Polymers via Inverse Vulcanization of Elemental Sulfur for Healable Infrared Optical Materials. *ACS Macro Letters* **4**, 862-866 (2015).

9. Xin Y, Peng H, Xu J, Zhang J. Ultrauniform Embedded Liquid Metal in Sulfur Polymers for Recyclable, Conductive, and Self-Healable Materials. *Adv Funct Mater* **29**, 1808989 (2019).

10. Yan P, *et al.* Inverse Vulcanized Polymers with Shape Memory, Enhanced Mechanical Properties, and Vitrimer Behavior. *Angew Chem Int Ed Engl* **59**, 13371-13378 (2020).

11. Hasell T, Yan P, Zhao W, Tonkin S, Chalker J, Schiller T. Stretchable and durable inverse vulcanized polymers with chemical and thermal recycling. (2021).

12. Crockett MP, *et al.* Sulfur-Limonene Polysulfide: A Material Synthesized Entirely from Industrial By-Products and Its Use in Removing Toxic Metals from Water and Soil. *Angew Chem Int Ed Engl* **55**, 1714-1718 (2016).

13. Lee J-Sing M, Parker DJ, Cooper AI, Hasell T. High surface area sulfur-doped microporous carbons from inverse vulcanised polymers. *J Mater Chem A* **5**, 18603-18609 (2017).

14. Scheiger JM, *et al.* Inverse Vulcanization of Styrylethyltrimethoxysilane-Coated Surfaces, Particles, and Crosslinked Materials. *Angew Chem Int Ed Engl* **59**, 18639-18645 (2020).

15. Petcher S, Zhang B, Hasell T. Mesoporous knitted inverse vulcanised polymers. *Chemical Communications* **57**, 5059-5062 (2021).

16. Deng Z, Hoefling A, Théato P, Lienkamp K. Surface properties and antimicrobial activity of poly (sulfur-co-1, 3-diisopropenylbenzene) copolymers. *Macromol Chem Phys* **219**, 1700497 (2018).

17. Smith JA, *et al.* Investigating the antibacterial properties of inverse vulcanized sulfur polymers. *ACS omega* **5**, 5229-5234 (2020).

18. Dop RA, Neill DR, Hasell T. Antibacterial Activity of Inverse Vulcanized Polymers. *Biomacromolecules*, (2021).

19. Worthington MJH, Kucera RL, Chalker JM. Green chemistry and polymers made from sulfur. *Green Chem* **19**, 2748-2761 (2017).

20. Zhang Y, Glass RS, Char K, Pyun J. Recent advances in the polymerization of elemental sulphur, inverse vulcanization and methods to obtain functional Chalcogenide Hybrid Inorganic/Organic Polymers (CHIPs). *Polym Chem* **10**, 4078-4105 (2019).

21. Tonkin SJ, *et al.* Chemically induced repair, adhesion, and recycling of polymers made by inverse vulcanization. *Chem Sci* **11**, 5537-5546 (2020).

22. Parker D, *et al.* Low cost and renewable sulfur-polymers by inverse vulcanisation, and their potential for mercury capture. *J Mater Chem A* **5**, 11682-11692 (2017).

23. Arslan M, Kiskan B, Yagci Y. Combining elemental sulfur with polybenzoxazines via inverse vulcanization. *Macromolecules* **49**, 767-773 (2016).

24. Wu X, *et al.* Catalytic inverse vulcanization. *Nature communications* **10**, 1-9 (2019).

25. Zhang B, Gao H, Yan P, Petcher S, Hasell T. Inverse vulcanization below the melting point of sulfur. *Materials Chemistry Frontiers* **4**, 669-675 (2020).

26. Takacs L. The historical development of mechanochemistry. *Chem Soc Rev* **42**, 7649-7659 (2013).

27. Friscic T, Mottillo C, Titi HM. Mechanochemistry for Synthesis. *Angew Chem Int Ed Engl* **59**, 1018-1029 (2020).

28. Szczęśniak B, Borysiuk S, Choma J, Jaroniec M. Mechanochemical synthesis of highly porous materials. *Materials Horizons* **7**, 1457-1473 (2020).

29. Mateti S, *et al.* Mechanochemistry: A force in disguise and conditional effects towards chemical reactions. *Chem Commun (Camb)* **57**, 1080-1092 (2021).

30. James SL, *et al.* Mechanochemistry: opportunities for new and cleaner synthesis. *Chemical Society Reviews* **41**, 413-447 (2012).

31. Kubota K, Pang Y, Miura A, Ito H. Redox reactions of small organic molecules using ball milling and piezoelectric materials. *Science* **366**, 1500-1504 (2019).

32. Baláž P, Baláž M, Achimovičová M, Bujňáková Z, Dutková E. Chalcogenide mechanochemistry in materials science: insight into synthesis and applications (a review). *Journal of Materials Science* **52**, 11851-11890 (2017).

33. Baláž P. Applied Mechanochemistry. In: *Mechanochemistry in Nanoscience and Minerals Engineering*). Springer Berlin Heidelberg (2008).

34. Friščić T. New opportunities for materials synthesis using mechanochemistry. *Journal of Materials Chemistry* **20**, 7599-7605 (2010).

35. Zhu S-E, Li F, Wang G-W. Mechanochemistry of fullerenes and related materials. *Chemical Society Reviews* **42**, 7535-7570 (2013).

36. Khan M, *et al.* Surface characterization of poly (3, 4-ethylenedioxythiophene)-coated latexes by X-ray photoelectron spectroscopy. *Langmuir* **16**, 4171-4179 (2000).

37. Ren Z, Jiang X, Liu L, Yin C, Wang S, Yang X. Modification of high-sulfur polymer using a mixture porogen and its application as advanced adsorbents for Au (III) from wastewater. *J Mol Liq* **328**, 115437 (2021).

38. Lisowska-Oleksiak A, Nowak A, Wilamowska M, Sikora M, Szczerba W, Kapusta C. Ex situ XANES, XPS and Raman studies of poly (3, 4-ethylenedioxythiophene) modified by iron hexacyanoferrate. *Synthetic metals* **160**, 1234-1240 (2010).

39. Ye J, He F, Nie J, Cao Y, Yang H, Ai X. Sulfur/carbon nanocomposite-filled polyacrylonitrile nanofibers as a long life and high capacity cathode for lithium–sulfur batteries. *J Mater Chem A* **3**, 7406-7412 (2015).

40. Petcher S, Parker DJ, Hasell T. Macroporous sulfur polymers from a sodium chloride porogen—a low cost, versatile remediation material. *Environ Sci Water Res Technol* **5**, 2142-2149 (2019).

41. Parker DJ, Chong ST, Hasell T. Sustainable inverse-vulcanised sulfur polymers. *RSC Adv* **8**, 27892-27899 (2018).

42. Lee JM, *et al.* Synthesis of poly (phenylene polysulfide) networks from elemental sulfur and p-diiodobenzene for stretchable, healable, and reprocessable infrared optical applications. *ACS Macro Lett* **8**, 912-916 (2019).

43. Zhang S, Pan L, Xia L, Sun Y, Liu X. Dynamic polysulfide shape memory networks derived from elemental sulfur and their dual thermo-/photo-induced solid-state plasticity. *Reactive and Functional Polymers* **121**, 8-14 (2017).

44. Lee T, Dirlam PT, Njardarson JT, Glass RS, Pyun J. Polymerizations with Elemental Sulfur: From Petroleum Refining to Polymeric Materials. *Journal of the American Chemical Society*, (2021).

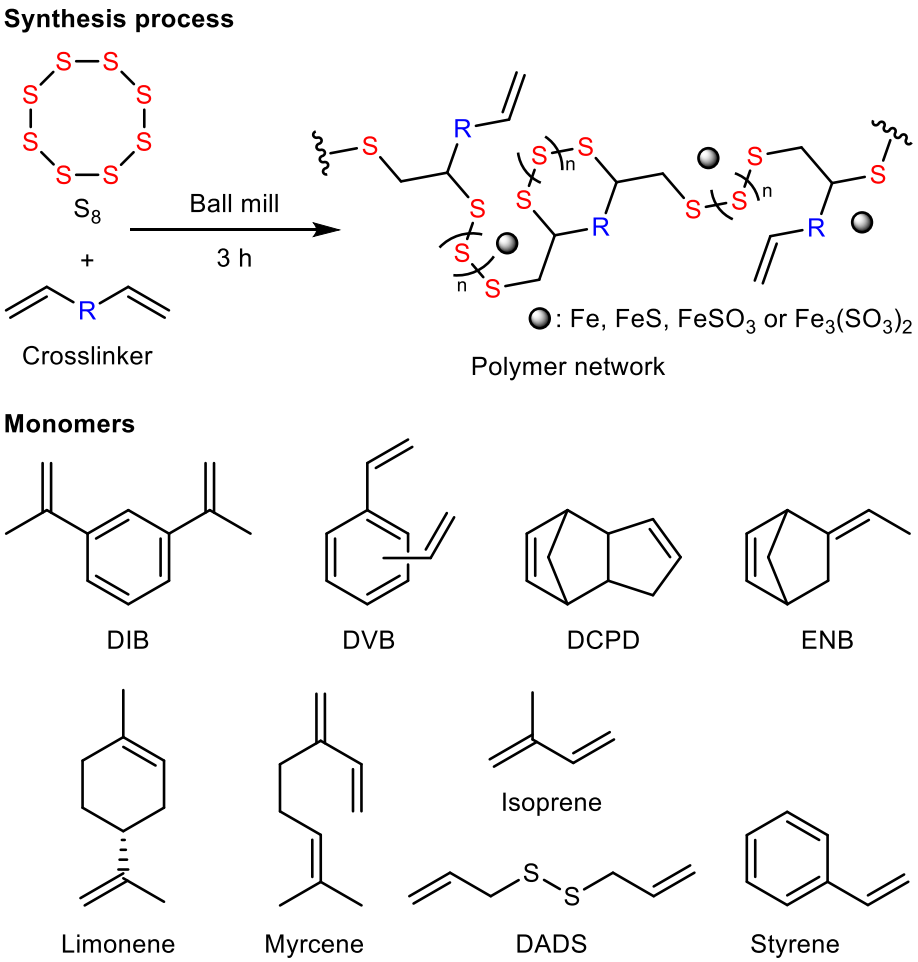

Fig. 1. Reaction scheme of MS of inverse vulcanized polymers and monomers used.

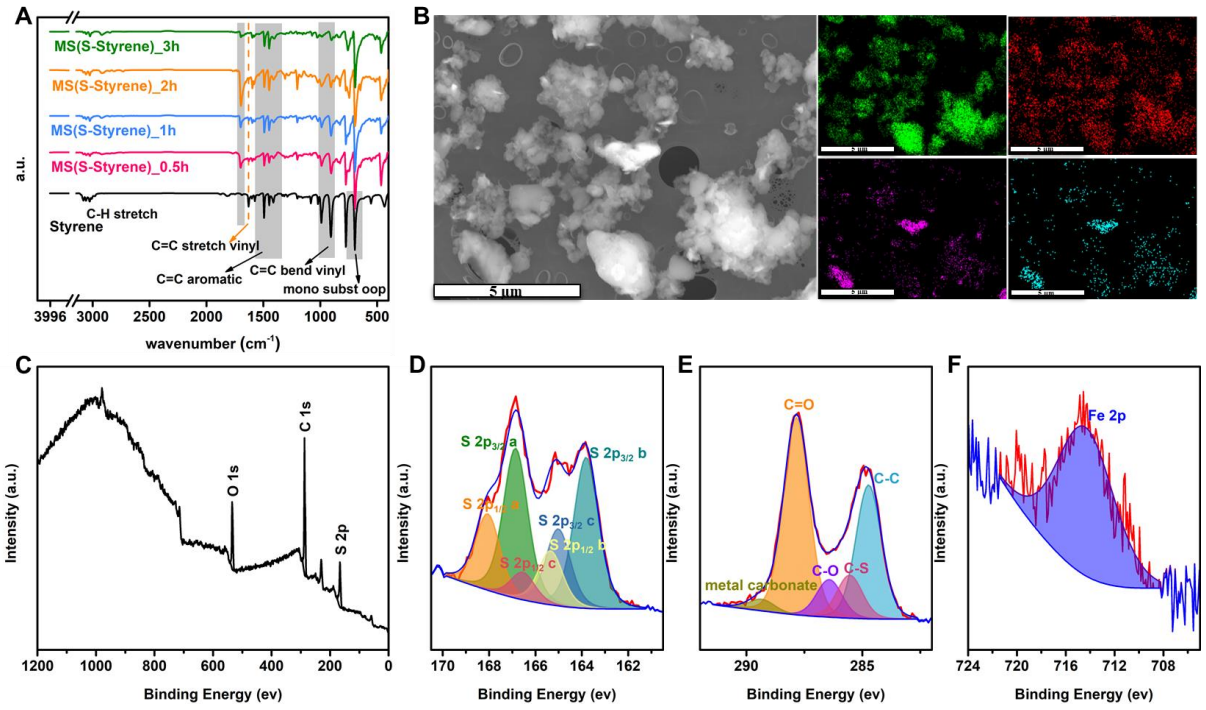

Fig. 2. A) Synthesis of MS(S-Styrene) monitored by using FT-IR. B) SEM and EDS images of product MS(S-DIB) with same size bar (5 µm). Panels C) to F) show XPS spectra of MS(S-Styrene); wide scan, and corresponding S 2p, C 1s, and Fe 2p spectra with associated curve fits.

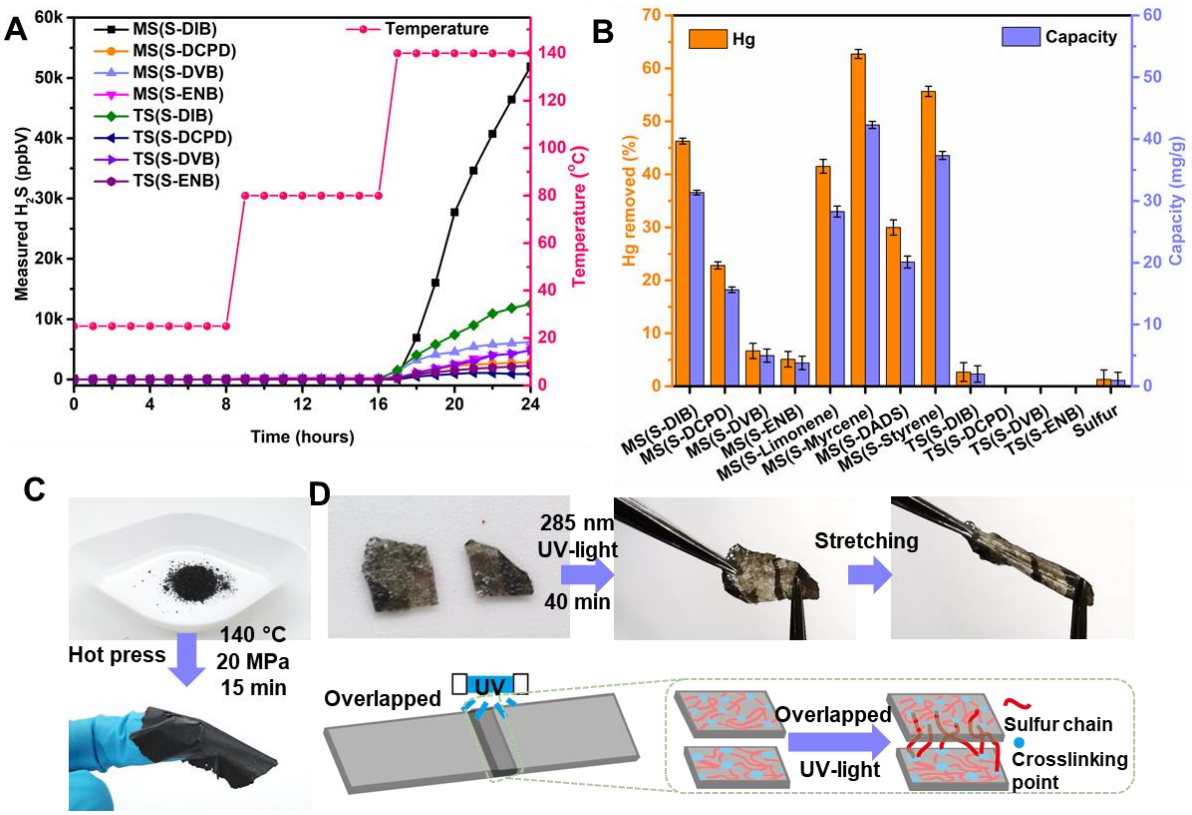

Fig. 3. A) H_2S measurements on selected MS and TS polymers with ramping temperature at room temperature, 80 °C and 140 °C. B) The percentage mercury removed in solution after 24 hours exposure to each of the materials listed. C) The capacity of mercury removing of each of the materials listed. D) Polymer MS(S-DIB) as an example to show the polymer film is able to be made from polymer powder. E) Polymer MS(S-ENB) film as an example to show the UV-induced self-healing ability of the MS polymer.

TOC:

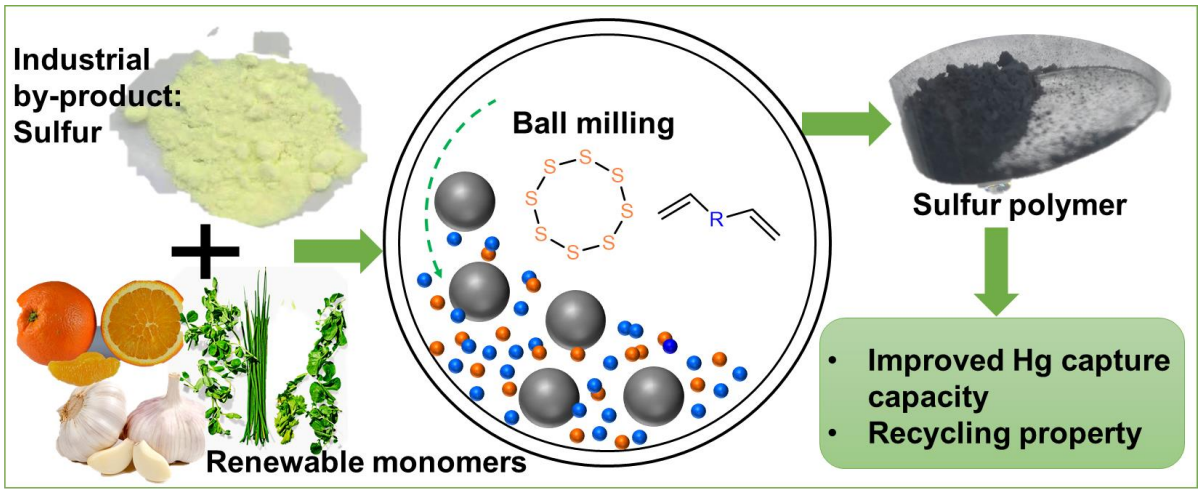
Industrial
by-product:
Sulfur
Renewable monomers
Ball milling
R
Sulfur polymer
• Improved Hg capture capacity
• Recycling property